phys. stat. sol. (b) **207**, 153 (1998)

Subject classification: 68.35.Bs; 66.30.Fq; 68.35.Ja; S1.3

Dynamics of Adatom Self-Diffusion and Island Morphology Evolution at a Cu(100) Surface

QIAN XIE[1])

Max-Planck-Institut für Physik komplexer Systeme, Nöthnitzer Str. 38, D-01187 Dresden, Germany

(Received November 4, 1997; in revised form January 27, 1998)

Molecular dynamics simulation of adatom self-diffusion and island morphology evolution at a Cu(100) surface is performed with the aim of a better understanding of the dynamical process. The simulation is at first carried out for a surface without adatoms or islands, and the vibrational spectra of the surface layers at different temperatures are calculated. We then add adatoms and islands to the surface, and perform simulations for systems with different surface structures. Based on the simulation results for a single adatom, we discuss a resonance mechanism possibly by which the adatom diffusion is activated by the surface vibration. The simulation results of an ad-dimer show a dancing motion of the dimer when it is about to dissociate. Finally we study the morphology of an island at finite temperatures. Our simulation results suggest that the exchange diffusion mechanism plays an important role on reshaping the island.

1. Introduction

Structure formation at a surface has attracted interest recently because of its importance to crystal growth [1]. Efforts have been made on ab initio electronic structure or semiempirical calculations of the energetics of atom migration and structure formation at a surface [2,3]. However, less attention has been paid to the study of dynamical processes, which is of equal importance in understanding the physics at a surface.

Adatom self-diffusion is believed to be of fundamental importance because it determines the surface morphology during expitaxial growth. In order to control the growing process we have to learn how to control the self-diffusion of adatoms. At low temperature or within a short time, an adatom is seen vibrating in the vicinity of an adsorption site. When the temperature is high or the time is long enough, it may migrate elsewhere. Two pathways for the adatom self-diffusion have been well established. One is called the hopping mechanism, the other the exchange mechanism. The latter is believed to be favored for Al(100) [4], Pt(100) [5], Ir(100) [6], and Cu(100) [7].

The standard picture for adatom self-diffusion is that the adatom overcomes the energy barrier which prevents it from leaving a stable position. The diffusion rate can thus be given by using the transition state theory, and the diffusion coefficient is believed to follow the Arrhenius law if the substrate does not undergo a significant structural transformation when the temperature rises. However, the dynamical process of the diffusion event remains unclear. It is explained in textbooks that the driving force of diffusion comes from the thermal activation. But what is the thermal activation,

[1]) Present address: Department of Natural Sciences, University of Cyprus, P.O. Box 537, CY 1678, Nicosia, Cyprus.

where does it comes from, and how does it make an individual diffusion event possible? Although it is very easy to produce a "live" diffusion event by the deterministic molecular dynamics method, these problems seem just too difficult to be answered by simulation methods.

But one thing is clear: It is the vibration of the substrate that provides the adatom the energy needed to move away. We know that a diffusion event is not possible at zero temperature when there is no substrate motion and the probability of diffusion increases when the temperature rises and the vibrational amplitude of the substrate consquently enlarges. But how does the substrate vibration activate the adatom? And how does diffusion change the landscape of an island at a surface?

This paper is aimed at a better understanding of these problems, with the assistance of molecular dynamics (MD) simulation. It is organized as follows. In Section 2, we briefly describe the interaction potential model and MD method employed in the present study. In Section 3, the simulation results for a surface without preset adatoms and islands are presented. In Section 4, we discuss a resonance mechanism, which may be helpful to understand adatom self-diffusion. In Section 5, the dissociation of an addimer is simulated. In Section 6, evolution of island morphology at finite temperature is shown. In Section 7, we conclude the paper with some discussions.

2. The Model and Simulation Method

To mimic a (100) surface of a f.c.c. crystal, a slab model is used. The mass center of the slab is placed at the center of the simulation box. Above and below the slab is vacuum. Periodic boundary conditions are used to extend the system to infinity, and the minimum image convention to calculate the force. The slab contains an odd number of atomic layers, with the central layer in the $z = 0$ plane. The layers above and below the central one are mirror images of each other, adatoms or islands are added to the adsorption sites of one surface and their mirror sites at the opposite surface, thus the two surfaces of the slab are geometrically equivalent. Initial velocities of the atoms are assigned according to the Maxwell distribution at a given temperature and shifted to ensure that the velocity of the center-of-mass of the system vanishes (in order to prevent the slab from drifting in the simulation box).

The Gear five-value predictor-corrector method [8] is used to integrate the Newtonian equations of motion. The time step is chosen to be 0.01 ps or less. Temperature control is applied when the system is being equilibrated. In the present work, the size of the box is fixed. Allowing the box shape to fluctuate may not bring much change to the surface properties since the surface is free in the perpendicular direction.

The embedded-atom method (EAM) [9,10] is employed to define a Cu sample. According to the EAM, the total potential energy of the system can be written as

$$V_{\text{tot}} = \tfrac{1}{2}\sum_i \sum_{j\neq i} \varphi_{ij}(R_{ij}) + \sum_i F_i\left[\sum_{j\neq i} \varrho_j(R_{ij})\right], \tag{1}$$

where R_{ij} is the interatomic distance between the atoms i and j, φ_{ij} the repulsive pair potential between i and j, ϱ_i the electron density for the atom i, and F_i the embedding function which describes the interaction between the atom and electron background. The functions for the pair potential and electron density are parametrized, with the use of the lattice inversion method [11], by which the equations selected to fit the param-

eters from the experimental data can be linearized [12]. Compared with the conventional fitting procedure, the scheme avoids the arbitariness for the determination of long-range potential functions. The potentials are able to satisfactorily reproduce a variety of material properties such as phase stabilities, elastic constants, phonon dispersions, structure factor, surface tensions of low-index surfaces and adsorption energy. The bulk melting point of Cu is predicted to be (1050 ± 50) K by using the constant-volume–temperature MD method and considerably underestimated to be (750 ± 50) K by using Andersen's constant-pressuretemperature MD method [8]. Nevertheless, the capability of the EAM potential to reproduce experimental results is not so important in this paper since what we are interested in is the dynamics of the system rather than the accuracy of the physical properties produced.

3. Surface Vibration and Premelting

The dynamics and phase transition of a surface are different from those of a bulk due to the discontinuity at the surface. Because they experience a smaller binding force, the atoms at a surface are more mobile than those in the bulk, thus, localized surface vibrational modes can be expected. Within the harmonic approximation, some of these modes correspond to the Rayleigh waves [13].

It is well-known that the surface premelts when the temperature is still below the bulk melting point [14]. The surface premelting of a (110) surface has been simulated by using molecular dynamics with the Lennard-Jones potential [15]. But a detailed dynamical behavior was not investigated in that work. As a matter of fact, a model system like the premolten surface can be suitable for the investigation of the crossover between lattice dynamics and phase transition. At a premelting temperature, a solid–liquid coexistence can be observed: Some surface layers are molten while the layers

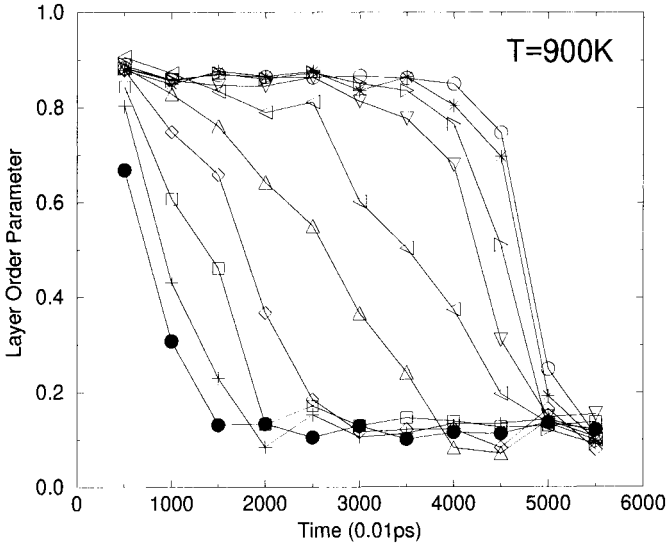

Fig. 1. Domino effect of the local order parameters for the layers at a premelting temperature. The filled circles denote the order parameter of the first toppest layer, and other symbols those of the gradually deeper layers

below them remain in a solid state. We can learn from such a system what makes the difference between a liquid and solid since both of these phases coexist at thermal equilibrium. An interesting problem is whether the solid–liquid interface exhibits some localized vibrational behavior due to the structural discontinuity across the interface.

We present some simulation results for a structureless surface in this section. The size of the slab is chosen to be $5a_e \times 5a_e \times 10a_e$, namely, there are 21 layers and each layer contains 50 atoms. The time dependent translational order parameter of the L-th layer is defined by an origin independent form

$$O_L(t) = \left\{\frac{1}{N_L}\sum_{i\in L}\cos\left[\mathbf{K}\cdot\mathbf{R}_i(t)\right]\right\}^2 + \left\{\frac{1}{N_L}\sum_{i\in L}\sin\left[\mathbf{K}\cdot\mathbf{R}_i(t)\right]\right\}^2, \tag{2}$$

where $\mathbf{K} = 2\pi/a(-1,1)$ for f.c.c. (100), $\mathbf{R}_i(t)$ is the position vector of the atom i which belongs to the layer at time t, and N_L is the number of atoms of the layer. It is shown in Fig. 1 that beginning from the top layer, the layers melt down one by one exhibiting a phenomenon, like the domino effect. After approximately 50 ps, the whole slab is molten. The propogation rate of the melting front is about 30 m/s, much smaller than the sound velocity in copper.

The thermal-equilibrium order parameters at different temperatures are calculated by averaging over 10 ps. It is shown in Fig. 2 that at 800 K solidliquid coexistence occurs: The toppest two layers are premolten while the others remain solid. This provides us a very good prototype to study the dynamical difference between a liquid and solid.

As the reader may have noticed, it is important to define a layer in a simulation before calculating its properties. One possible definition is to cut the slab along the perpendicular direction into a number of slices and averaging the local physical properties over the atoms which belong to the same slice. This treatment is complicated. Instead, we sort the atoms into different sets by layers according to the initial configuration, and the properties are calculated on the basis of these sets. The atoms of a set

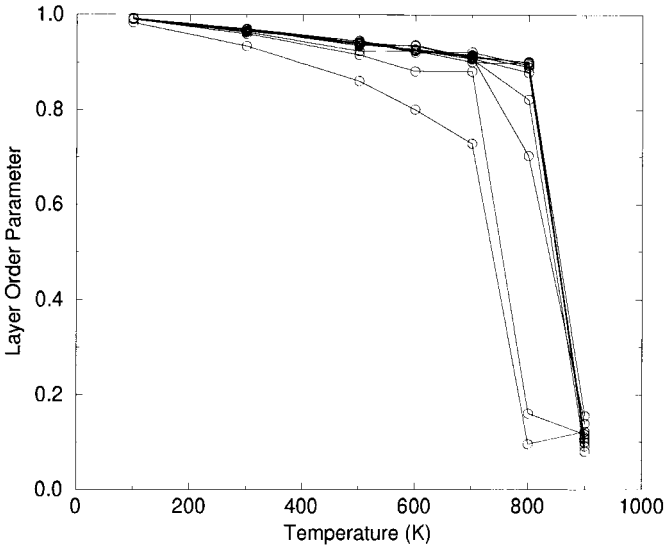

Fig. 2. Equilibrium order parameters for the toppest ten layers (open circles) versus temperature

may not be actually confined within the Gaussian spread of a layer during the simulation, due to interlayer diffusion which becomes more active at a higher temperature, however, the problem of interlayer diffusion may not matter too much at low and high temperature limits. When the temperature is low, the diffusivity is low and the conformation of the sets does not differ too much from layered structure in the time scale of a simulation. When the temperature is above the premelting point, the motion of the atoms is completely random, all the atoms in the slab become statistically equivalent, and the properties averaged over a former set should be close to those averaged over the whole slab if the number of atoms belong to it is large enough. At other temperatures, we have to check if the conformations deviate largely from a plane. The deviation of a conformation from a plane is defined by

$$\Delta_L = \left\langle \sqrt{\frac{1}{N_L} \sum_{i \in L} (z_i - \overline{z}_L)^2} \right\rangle_t , \tag{3}$$

where $\overline{z}_L$ is the average of the z coordinates of all the atoms in the layer L, $\langle \rangle_t$ the time average over a run. Fig. 3 shows the equilibrium deviations for the layers at different temperatures. It is found that the deviation for a solid-state layer is very small, suggesting the interlayer diffusion in solid state is not notable in the simulation time scale. At 800 K, Δ_1 and Δ_2 significantly increase to a high level, implying that the atomic diffusion in the direction perpendicular to the surface is very active in the premolten layers. Δ_3, the deviation of the solid–liquid interface, also shows a drastic increasing. However, those for the solid-state layers are not affected by the premelting of the top two layers. The enlargement of them seems to be caused solely by the rising of temperature. This means that there is no significant interphase diffusion across the interface in the simulation time scale. Diffusion of an atom from the solid phase to the liquid phase may happen, but such an event does not bring significant error to the physical properties

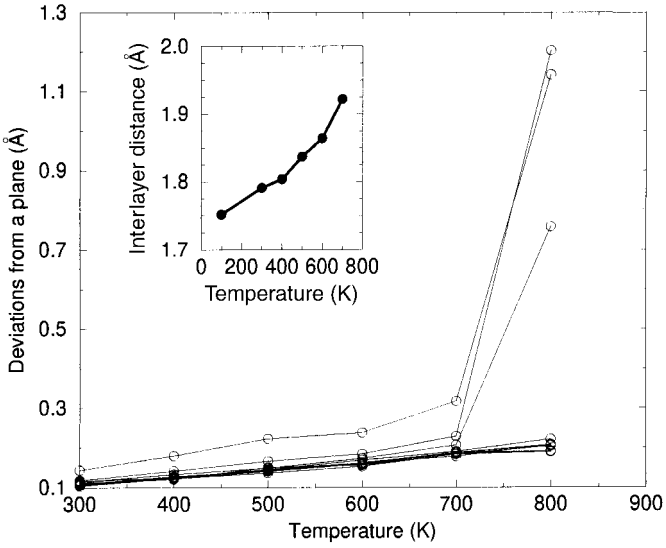

Fig. 3. Deviations of the layers from a plane. The inset shows the thermal expansion of the top layer

evaluated by averaging over the original sets, because the majority of the atoms in the set remain near their starting positions and the error is caused by only a few outgoing atoms (hence it is minor). However, this conclusion is not correct for very long time simulation, since slow diffusion can after all change the landscape finally.

The local velocity–velocity autocorrelation function (VVACF) of the L-th layer in different orientations is defined by

$$C^{(L)}_{V_\alpha V_\alpha}(t) = \frac{1}{N_L} \sum_{i \in L} \langle \mathbf{V}_{i\alpha}(t) \cdot \mathbf{V}_{i\alpha}(0) \rangle / \langle \mathbf{V}_{i\alpha}(0) \cdot \mathbf{V}_{i\alpha}(0) \rangle \,, \tag{4}$$

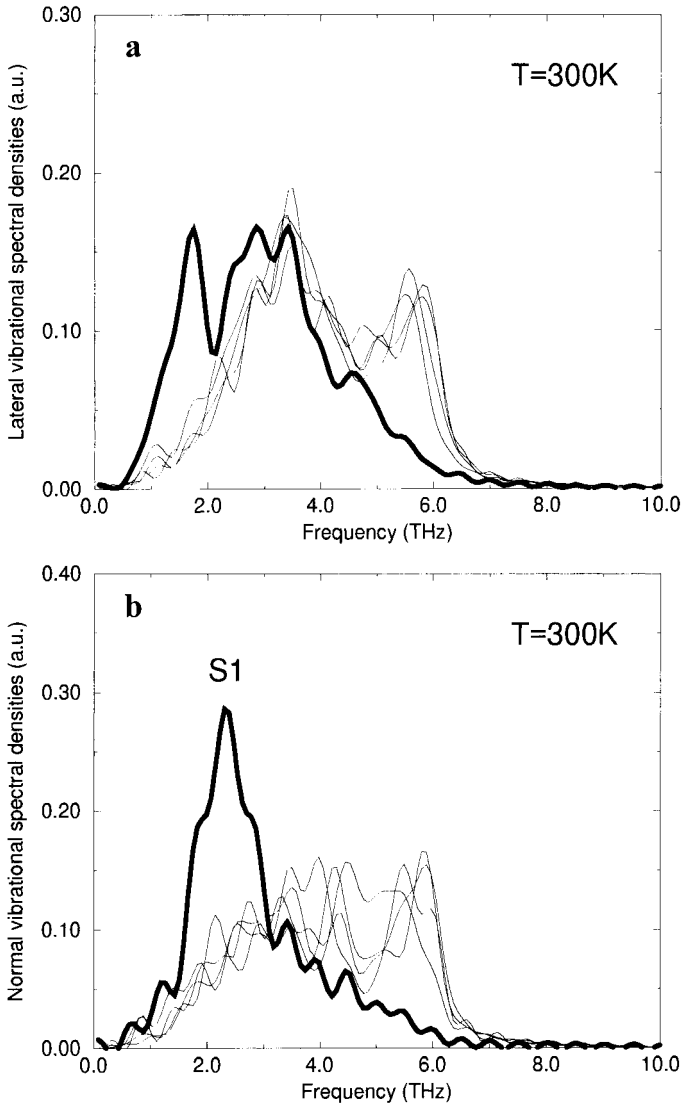

Fig. 4. a) Lateral and b) normal spectral densities (in arb. units) of the layers at 300 K. The solid lines denote the spectra of the first layer and the thin lines those of the other layers. The peak in the normal spectrum corresponds to the Rayleigh waves (S1)

where $\langle\,\rangle$ represents average over the starting time and α the direction. Total VVACFs are obtained by averaging over three directions $C_{VV} = (C_{V_xV_x} + C_{V_yV_y} + C_{V_zV_z})/3$.

The vibrational spectrum of a layer can be obtained by performing the Fourier transform on the VVACF of the layer. Fig. 4 shows the lateral and normal spectral densities of the layers at 300 K. Localized surface modes are observed in both directions. The major weight of the normal component redshifts to 2 to 3 THz, in agreement with the

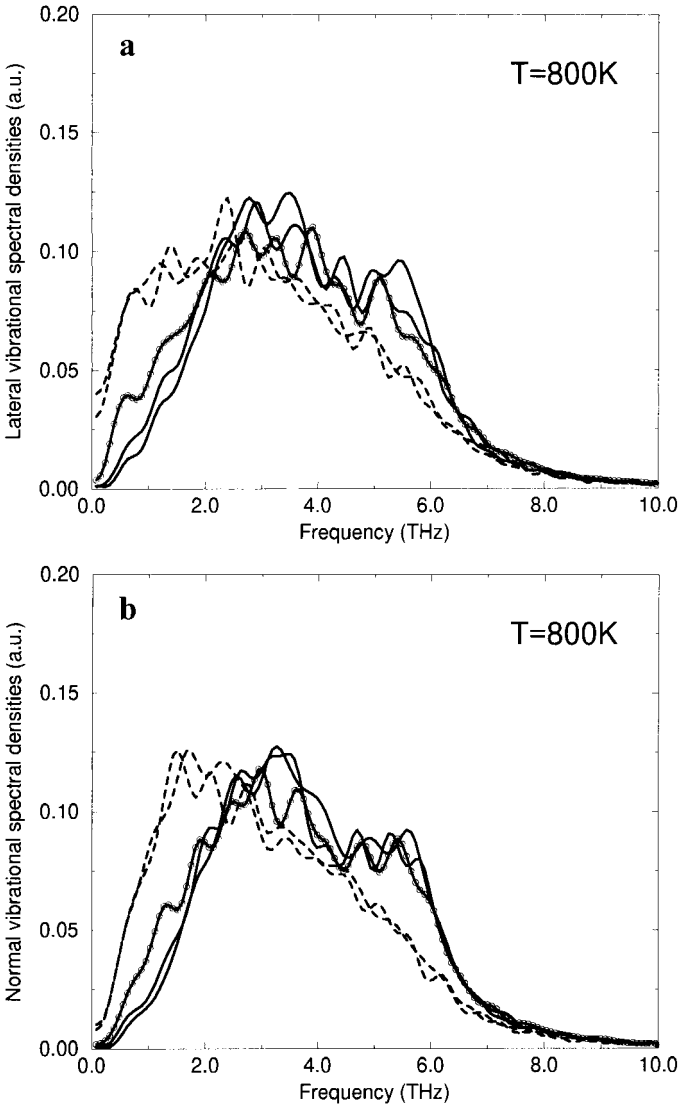

Fig. 5. a) Lateral and b) normal spectral densities of the layers for a coexisting solid–liquid slab. The dotted lines in a) and b) denote the corresponding functions of the toppest two liquid layers, the solid lines with small circles those of the solid–liquid interface, and the other solid lines those of the solid layers

recent result for Cu(100) by Kürpick et al. [16] using the real space Green function method. While the lateral component shows some redshift, it is after all more bulk-like. There is not much difference among the spectral densities of the inner layers and they are very similiar to that of a bulk.

At 800 K, a solid–liquid interface is created in our system. If we write the equations of motion for the atoms at the interface we will find that the equations will clearly have a boundary condition which can be imagined as a stochastic perturbation. Mathematically this problem will be interesting. Fig. 5 shows the lateral and normal spectral densi-

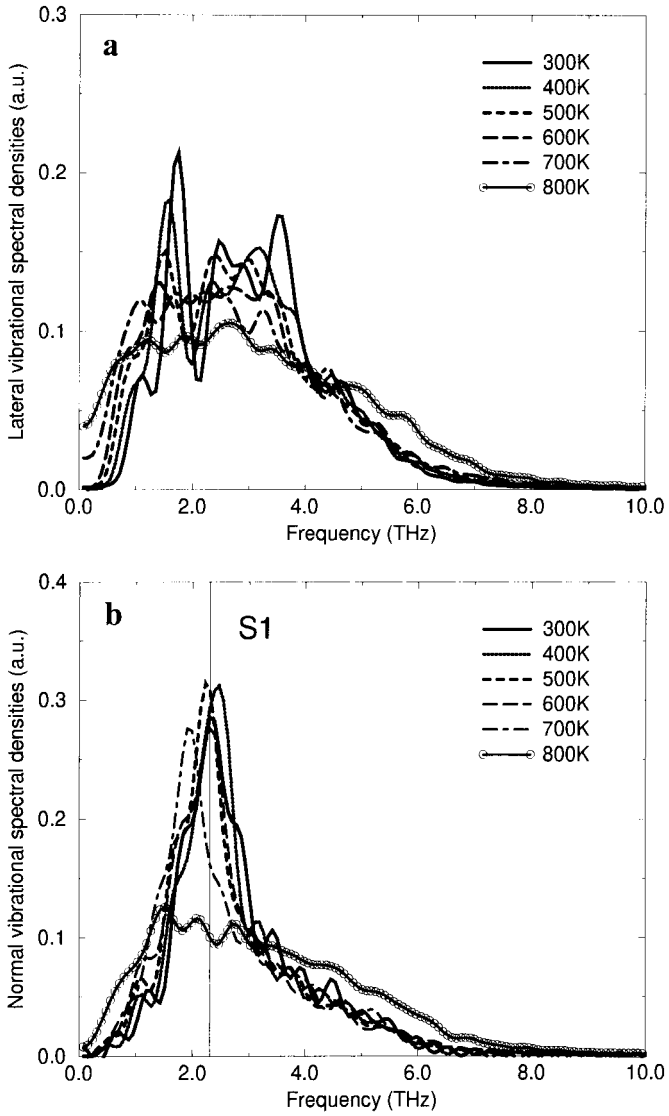

Fig. 6. a) Lateral and b) normal spectral densities at different temperatures, showing the critical behavior in the momentum space

ties of the layers at 800 K. It is found that the vibrational spectrum for the solid–liquid interface differs less from the solid layers than from the liquid ones. This implies that statistically the stochastic boundary might yield limited effect on localizing a vibrational mode.

We know that the critical behavior in the real space is that the order parameter suddenly vanishes at some temperature. It would be interesting to know what the critical behavior looks like in the momentum space. We examine the variation of the lateral and normal modes of the toppest layer with respect to the increasing temperature. Fig. 6 shows the spectra at different temperatures. It is found that the surface modes change as abruptly as does the order parameter when the temperature increases to a premelting point.

4. Dynamics of an Adatom: A Resonance Mechanism

A self-diffusion event is in fact a local phase transition (hence this problem may be as profound as the long-standing puzzle of melting dynamics). The driving force for such a local transition apparently comes from the interaction of the adatom with the substrate lattice. Kürpick et al. [16] have shown that the lattice vibration of the surface can be important to adatom mobility. They used the Green function method to calculate and compare the local densities of states for configurations in which the adatom sits at a fourfold site and the bridge site. The contribution from vibrational entropy to lowering the energy barrier can therefore be examined. However, their results seem not helpful in understanding the individual dynamical process. From the MD point of view, the energy barrier is not fixed in the time scale of a diffusion event due to the surface vibration. The vibrations of the adatom and surface are coupled due to the existence of their interaction. The difference of the vibrational frequencies of the adatom modes from those of the surface modes may promote a diffusion event in some part of a phonon time and inhabit it in the remaining time.

In this section, we suggest a resonance mechanism for adatom self-diffusion. As a very rough approximation, the adatom can be naively imagined as linked with the toppest layer of the surface by a spring k_1, the layer is installed on the rest of the solid by an array of springs k_2 (Fig. 7). We have known from the MD simulation that the normal mean square displacements averaged over the layers decay with respect to the depths of the layers. For simplicity, we assume that only the toppest layer has a nonvanishing oscillation amplitude A^z_{surf}, and the vibration of other layers is neglected. The difference between the stretching force constants of the springs k_1 and k_2, and hence that between the vibrational frequencies of the adatom and a layer atom, are actually determined by the difference of the coordination numbers (the number of nearest neighbors), if only the nearest neighbor interaction is considered. We further assume that the in-plane coupling between the surface atoms is particularly strong so that rippling of the surface layer is not allowed, namely, there is no phase difference among the normal oscillations of the surface atoms. This assumption is reasonable because we have seen in above section that the deviations of the surface layers from a plane are not significant at 300 K. According to this assumption, for the case of the (100) surface, the number of bonds affecting the normal vibration of the adatom is in fact the same as that affecting the normal vibration of a layer atom not being the immediate neighbors of the adatom, which equals to four (remember the in-plane bonds do not contribute to

the z component of the force constant). For those immediate neighbors, this number is five (so their vibrational frequencies will be slightly different from those of the other layer atoms), but this difference can be ignored, since we have assumed that the in-plane coupling between the layer atoms are so strong that all the atoms in the layer must move together. Thus, we transfer the complex system into a toy model of *forced oscillation*. If the surface layer vibrates like a harmonic oscillator with a frequency ν, then the vibrating amplitude in z direction of the adatom is

$$A^z_{\text{ad}} = A^z_{\text{surf}}/|\omega^2 - \nu^2|\,, \tag{5}$$

where ω is the vibrational frequency of the adatom. Equation (5) simply means that the closer the frequencies are, the larger the vibrating amplitude of the adatom is, when $\omega = \nu$ the resonance effect occurs. For a f.c.c. (100) surface, since $\omega \approx \nu$, it is plausible to expect that the resonance mechanism might be able to play a nontrivial role on adatom dynamics.

If a resonance-like mechanism does work, the amplitude of the adatom vibration will be much larger than that of the substrate vibration. We can conjecture that the activation energy is thus significantly given to the adatom by the surface vibration, which makes pretty chance for the adatom to overcome the diffusion barrier. In Fig. 7, we show that the hopping diffusion is favored when the adatom moves upwards while the exchange diffusion is favored when it moves downwards considering the fact that the neighboring atoms are displaced to make way for a concerted exchange motion.

The realistic diffusion process is certainly much more complicated than the above-mentioned model. The MD simulation method can help to examine to what extent the role of such a resonance mechanism may be serious. In our MD simulation, the adatom is originally placed at the four-fold hollow position. The calculated unrelaxed adsorption energy is 2.77 eV and the unrelaxed diffusion barrier 0.56 eV, a little larger than the experimental value 0.40 eV obtained by He-atom scattering experiment [16]. Conjugate-gradient minimization shows that the relaxed distance between the adatom and the surface is 1.70 Å, about 0.1 Å smaller than the interlayer distance. The relaxation energy is less than 0.1 eV. To check the resonance mechanism, first of all, we

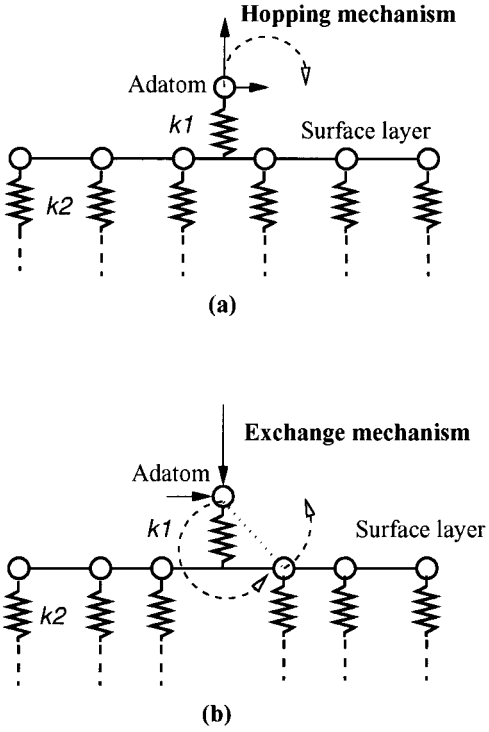

Fig. 7. Schematical illustration of a resonance mechanism for adatom diffusion, suggesting the importance of the normal vibration. a) A hopping diffusion is favored when the adatom moves upwards; b) an exchange diffusion is favored when the adatom moves downwards

have to examine the vibrational spectra. Fig. 8 shows the lateral and normal VVACFs and corresponding spectra of an adatom, in comparison with those of the atoms at different surface layers. The shape of the lateral component of the adatom spectrum is quite different from that of the lateral surface mode, while the difference between the normal component and the normal surface mode is less, the main peaks are comparably strong and close (in agreement with the results by the Green function method [16]).

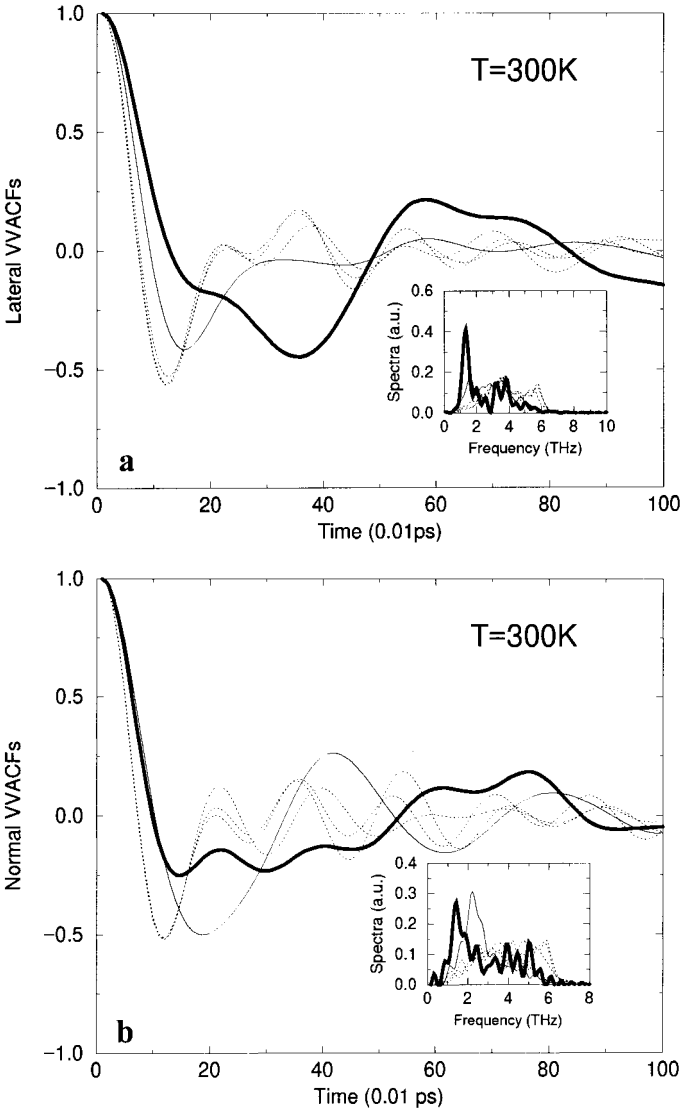

Fig. 8. a) Lateral and b) normal VVACFs and corresponding vibrational spectra of an adatom (solid lines), in comparison with those of the atoms at different surface layers (thin lines: top layer; dashed lines: other layers). The simulation temperature is 300 K. No diffusion event occurs in the simulation time. The insets are the corresponding spectra

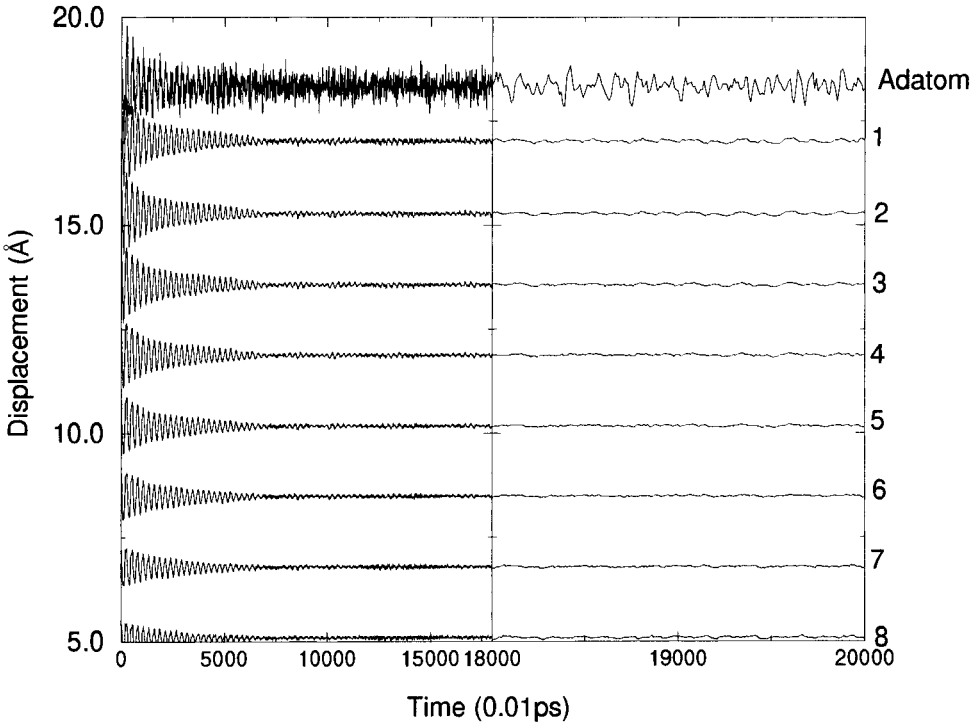

Fig. 9. Perpendicular displacement record of an adatom at 300 K, in comparison with those of the centers of mass of the surface layers. No diffusion event occurs in the simulation time

Second, we check the vibrational amplitude of the adatom. Fig. 9 illustrates the perpendicular displacements of the adatom and the centers-of-mass of the surface layers. The simulation is performed with an initial state in which the adatom and surface are at unrelaxed positions. Therefore, significant vibration of the layers is observed when the relaxation energy is released and transfered into kinetic energy. In the equilibration the temperature of the system is controlled by the rescaling method, so one can see that the vibration of the system is gradually damped. However, throughout the simulation the vibration of the adatom is obviously *not* damped. As a result, the amplitude of the adatom eventually becomes much larger than those of others after equilibration. Note that in the last section we have shown that the deviations of the layers from a plane are less than 0.2 Å at 300 K, it is safe to say that the amplitude of the adatom is much larger than those of the surface atoms.

5. Dissociation of an Ad-Dimer

The interaction of two adatoms is important for island formation. An ad-dimer can be regarded as the smallest island. Therefore, it is interesting to learn under what temperature and by which mechanism a dimer will be dissociated.

We know that there are two major mechanisms (hopping and exchange) for adatom self-diffusion. Correspondingly, we have two mechanisms for the dissociation of a dimer. One is that the adatoms leave each other by the hopping path, the other that one of them exchanges with a substrate atom which afterwards goes away.

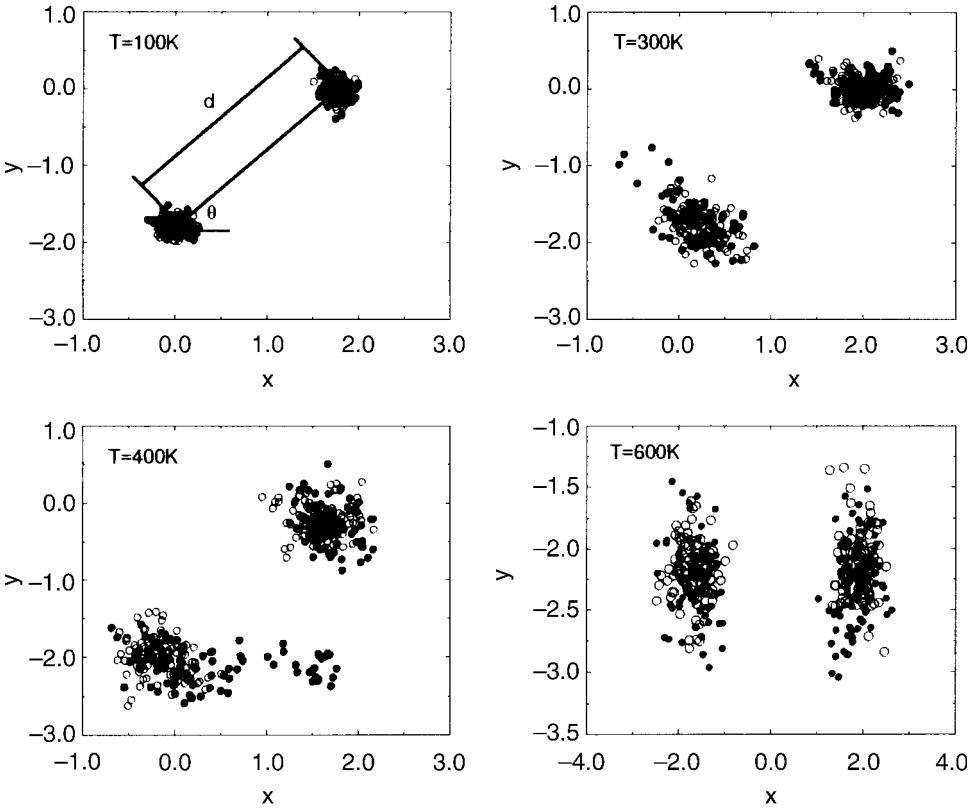

Fig. 10. Trajectory record for the dissociation of an ad-dimer. The open and filled circles denote the records of two successive runs. d in the first picture denotes the bond length and θ the orientation angle of the ad-dimer

In our simulations, two adatoms are put at two neighboring positions to form a dimer. A simple static calculation without considering relaxation effect shows that the binding energy of such a dimer is -0.37 eV. Care is taken that the dissociation process is not caused by the periodic boundary conditions. Simulation results (Figs. 10 and 11) show that at 600 K the dimer is still weakly bound with the equilibrium bond length equal to the next nearest neighbor distance. No exchange diffusion is observed for the ad-dimer in all the simulations. In Fig. 10, the trajectories of the two adatoms in two successive runs are shown, from which we can learn how the trajectories gradually deviate from that of a bound one when the temperature increases.

The dissociation dynamics of a dimer at 500 K is demonstrated in Fig. 12. Within the coordination system with origin at adatom a, adatom b is seen to have transited at positions II and III on its way to position IV, then it visits position IV for about 10 ps before staying at position III for 20 ps. After that, it returns to position IV and relatively stably resides there. Meanwhile, adatom a is also moving away from its orginal position. The resultant motion of the dimer looks like dancing (see the lower right panel of Fig. 10).

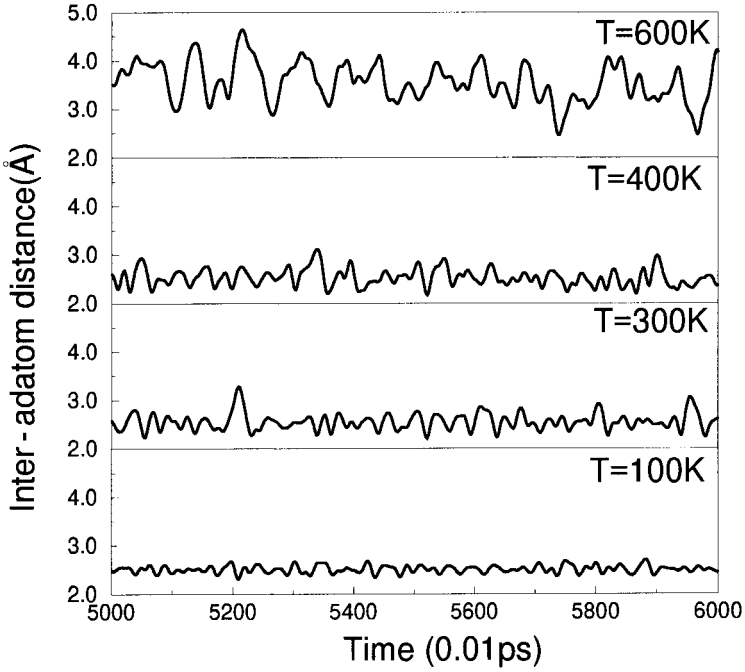

Fig. 11. Time evolution of the bond length of a dimer at different temperatures

6. Morphology of an Island at Finite Temperature

The morphology of an island at a surface has been studied by Voter [17] using arbitrary interatomic potentials and the lattice-gas kinetic Monte Carlo method, which is based on the transition state theory. The method requires knowledge of the states to which a system will evolve, but it is very possible that this knowledge is incomplete. As we have known, in addition to the two well-known mechanisms of surface self-diffusion, there may exist a mechanism for island dynamics by vacancy motion, which is recently proposed to explain some scanning tunneling microscopy pictures [18], and a dislocation mechanism, which is suggested for island migration based on the EAM calculation [19].

The natural method to study this problem is by MD simulation. However, the time scale of the conventional MD method is typically limited to a few nanoseconds or less, while many interesting problems such as Ostwald ripening of surface islands require a time scale of a few hours [18]. A recent progress towards large-time scale simulation is the hyperdynamics method put forward by Voter [20]. Nevertheless, he only demonstrated the evolution of an island with ten atoms in the time scale of 100 μs, which is far less than the time scale and system size for an Ostwald ripening simulation.

Because it is difficult to study the long-time dynamics of an island at present, we perform the MD simulation for a close-packed island with 64 atoms at 600 K in a time scale of nanoseconds. Since the ab initio step formation calculation suggests that the {111}-faceted step is energetically favored [3], we choose an island with the

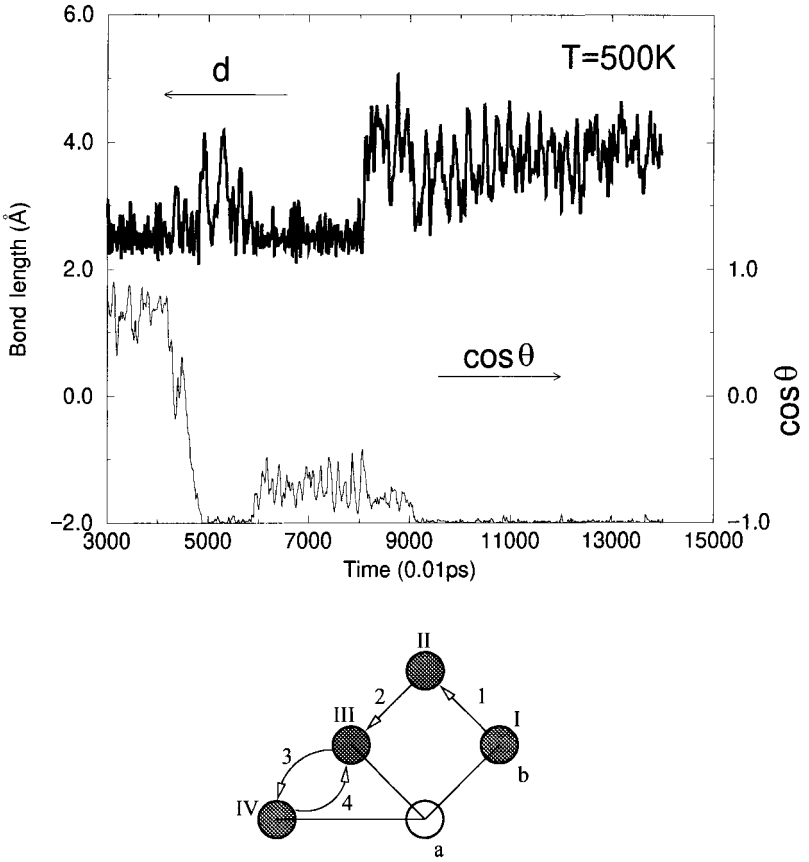

Fig. 12. Dissociation process of a dimer at 500 K. Shown are the time evolution of the bond length and orientation. The rotation of the dimer is also illustrated in the lower part

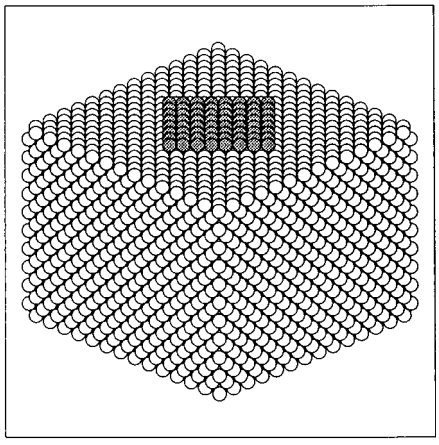

Fig. 13. Initial configuration of a one-layer close-packed island ({111}-faceted, 64 atoms). Island atoms are denoted by grey balls, while other atoms by white balls. There are 8232 atoms in the slab and 64 island atoms on each side of the slab

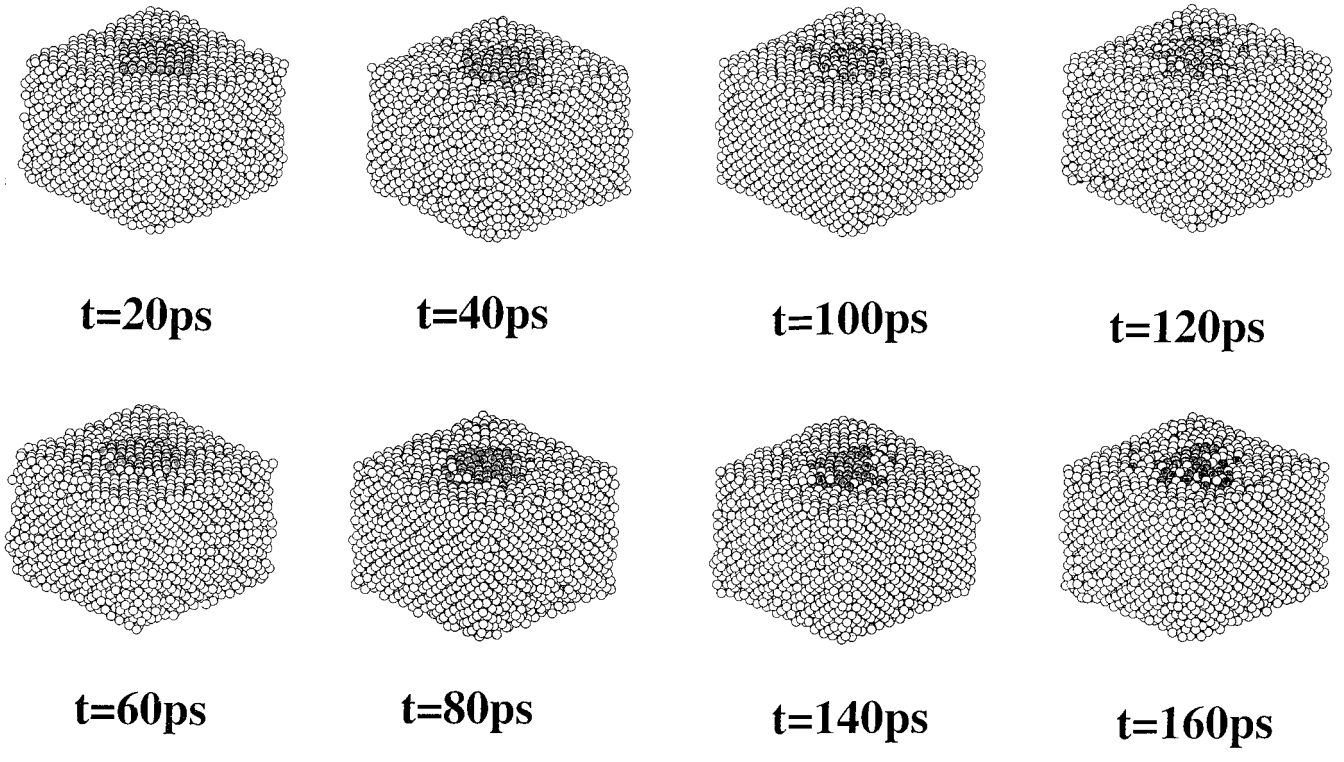

Fig. 14. Snapshots of the island every 20 ps during the simulation

whole boundary {111}-faceted as the starting configuration (see Fig. 13). At a time scale of a few nanoseconds, one may expect that the notable motion of the island is limited at the edges of the island and the center-of-mass of the island does not drift too much. (However, such drifts are necessary for the ripening dynamics.) Based on our simulation results, this is true. However, our results suggest that the edge-running mechanism [17] by which atoms run along the island edges is not true. Substantial exchange diffusions of edge atoms are observed throughout the simulation (Fig. 14).

7. Concluding Remarks

We have studied the dynamics of an adatom and island at a Cu(100) surface by using the MD simulation method with the EAM. A resonance mechanism of adatom dynamics is discussed based on the MD results, the dissociation of an ad-dimer is simulated, and the exchange diffusion is found important to the evolution of island morphology.

MD simulation may be able to produce limited informative results for the intriguing dynamics of highly nonlinear phenomena such as diffusion and melting. However, it may not be enough if we desire to get more details. Recent progress on the theory of lattice dynamics may provide something instructive. For example, it was discovered that in anharmonic lattices there exist intrinsic localized modes or discrete breathers which are time-periodic and localized in space [21]. They normally have a much higher energy than other modes and might be mobile. For a surface with a gap in the phonon dispersion spectrum, a breather may exist. It is therefore interesting to know what will happen if a travelling breather collides with an adatom. This mechanism may help to feed the adatom the activation energy to jump if the breather is destroyed by the collision and its energy absorbed by the adatom.

Acknowledgements The author would like to thank M. Antoni, S. Flach, G.X. Huang, S.P. Kashinje, and W.Q. Zhang for stimulating discussion, and the Max-Planck-Institute for Physics of Complex Systems for kind hospitality. The author is also grateful to Dr. G. Archontis for helping to correct some grammatical errors. This paper is dedicated to Prof. N.X. Chen on the occasion of his 60th birthday and the opening of the Laboratory of Virtual Materials Design.

References

[1] A.C. Levi and M. Kotrla, J. Phys.: Condensed Matter **9**, 299 (1997).
[2] C. Stampfl and M. Scheffler, Phys. Rev. Lett. **72**, 254 (1994); Phys. Rev. B **53**, 4958 (1996).
[3] B.D. Yu and M. Scheffler, Phys. Rev. Lett. **77**, 1095 (1996); Phys. Rev. B **55**, 13916 (1997).
[4] P.J. Feibelman, Phys. Rev. Lett. **65**, 729 (1990).
[5] G.L. Kellogg and P.J. Feibelman, Phys. Rev. Lett. **64**, 3143 (1990).
[6] C.L. Chen and T.T. Tsong, Phys. Rev. Lett. **64**, 3147 (1990).
[7] L. Hansen, P. Stoltze, K.W. Jacobsen, and J.K. Nørskov, Phys. Rev. B **44**, 6523 (1991).
[8] M.P. Allen and D.J. Tildesley, Computer Simulation of Liquids, Oxford University Press, New York 1987.
[9] M.S. Daw and M.I. Baskes, Phys. Rev. Lett. **50**, 1285 (1983); Phys. Rev. B **29**, 6443 (1984).
[10] M.S. Daw, S.M. Foiles, and M.I. Baskes, Mater. Sci. Rep. **9**, 251 (1993).
[11] N.X. Chen, Phys. Rev. Lett. **64**, 1193 (1990).
N.X. Chen, Z.D. Chen, and Y.C. Wei, Phys. Rev. E **55**, R5 (1997).

[12] QIAN XIE and MEICHUN HUANG, phys. stat. sol. (b) **186**, 393 (1994).
[13] M.C. DESJONQUÉres and D. SPANJAARD, Concepts in Surface Physics, Springer-Verlag, Berlin 1993 (p. 112).
[14] A. ZANGWILL, Physics at Surfaces, Cambridge University Press, 1988 (p. 119).
[15] V. ROSATO, G. CICCOTTI, and V. PONTIKIS, Phys. Rev. B **33**, 1860 (1986).
[16] U. KÜRPICK, A. KARA, and T.S. RAHMAN, Phys. Rev. Lett. **78**, 1086 (1997).
[17] A.F. VOTER, Phys. Rev. B **34**, 6819 (1986).
[18] J.B. HANNON, C. KLÜNKER, M. GIESEN, H. IBACH, N. C. BARTETT, and J. C. HAMILTON, Phys. Rev. Lett. **79**, 2506 (1997).
[19] J.C. HAMILTON, M.S. DAW, and S.M. FOILES, Phys. Rev. Lett. **74**, 2760 (1995).
[20] A.F. VOTER, Phys. Rev. Lett. **78**, 3908 (1997).
[21] A.J. SIEVERS and S. TAKENO, Phys. Rev. Lett. **61**, 970 (1988).
S. FLACH, Phys. Rep., to be published.